Facile Method of Preparing Supertough Polyamide 6 with Low Rubber Content

Zhuo Ke,[†] Dean Shi,*[,‡] Jinghua Yin,*[,†] Robert K. Y. Li,[§] and Yiu-Wing Mai[||]

State Key Laboratory of Polymer Physics and Chemistry, Changchun Institute of Applied Chemistry, Chinese Academy of Sciences, Graduate University of Chinese Academy of Sciences, Changchun 130022, P. R. China; Faculty of Materials Science and Engineering, Hubei University, 430062, Wuhan, P. R. China; Department of Physics and Materials Science, City University of Hong Kong, Tat Chee Avenue, Kowloon, Hong Kong, P. R. China; and Centre for Advanced Materials Technology (CAMT), School of Aerospace, Mechanical and Mechatronic Engineering (J07), The University of Sydney, Sydney, NSW 2006, Australia

Received March 5, 2008
Revised Manuscript Received September 17, 2008

The impact performance of semicrystalline polymers including polyamides can be greatly enhanced by adding rubber fillers.[1−3] Strong toughening is achieved when the rubber phase forms a submicron-sized dispersion which is usually obtained by reactive blending.[3−5] Experimental[6−11] and theoretical[12−14] studies show that the role of rubber in toughening of semicrystalline polymers is mainly related to the cavitation of rubber. The high dilative stresses in front of a growing crack promote the formation of voids in or around rubber particles. Thus, the hydrostatic pressure is relieved near the voids, and stresses are redistributed in a cellular-like material. Cavitated particles act as stress raisers around which the polymer matrix deforms plastically. However, for this toughening method to work, a substantial rubber concentration of about 10−20 wt % is required. Wu[7] found that toughening can only be achieved below a critical interparticle ligament thickness, L_C, which is generally considered as an intrinsic property of the matrix, independent of the size and nature of particles. However, many previous works reported that the nature of the rubber and the matrix, the morphology of the dispersed phase (i.e., rubber particle size and its distribution), rubber content, and processing conditions are important factors that determine the level of toughening of polyamides.[15−19] Recently, Corté and Leibler[20] proposed a different model for semicrystalline polymers toughened by rubber particles based on two competing processes of matrix shear yielding activated by the particles and of brittle fracture caused by coalescence of microcracks between crystalline lamellae. They showed that for successful toughening the interparticle distance L should be smaller than a critical length L_C, which is given by

$$L_C = \xi^* + d\left(\frac{C\sigma_B}{\sigma_Y}\right)^2 \quad (1)$$

where ξ^* is the mean distance between microcracks, σ_B the characteristic matrix brittle fracture stress usually measured at low temperature or high speed, σ_Y the matrix tensile yield stress, d the average size of dispersed particles, and C a coefficient related to the cavitation capability of the particles and the brittle fracture criterion.[20] Equation 1 shows that the critical distance L_C depends not only on the matrix characteristics given by ξ^*, σ_B, and σ_Y but also on particle size d. If we ignore the particle size distribution and assume the particles are arranged in a cubic lattice, then the ligament thickness L is related to d and dispersed volume fraction Φ by $L = d[(\beta\pi/6\Phi)^{1/3} - 1]$, where β is a geometry factor close to unity.[7] Thus, the minimum filler volume fraction for onset of ductility or toughness can be obtained from

For a given polymer matrix, one possible way to reduce the

$$\Phi_C = \frac{\beta\pi}{6}\left(1 + \frac{\xi^*}{d} + \left(\frac{C\sigma_B}{\sigma_Y}\right)^2\right)^{-3} \quad (2)$$

critical rubber volume fraction Φ_C is to decrease the particle size d. But, in practice, d must be large enough to ensure cavitation occurs so as to relieve the local hydrostatic stress and initiate matrix shear yielding.[21] Hence, a large amount of rubber (e.g., ∼10−20 wt %) is required to obtain high toughness. To overcome this problem, polymer/elastomer/filler ternary systems[22−25] or block copolymers with both glassy and rubbery blocks,[15,16,26−29] rather than pure rubber, are used to improve the toughness. In these systems, the formation of a core−shell structure with rigid core and soft rubber shell is needed to achieve high toughness with low rubber content.[30−32] For example, the rubber content can be reduced to 7 wt % in polyamide 12 toughened with PS−PB−PMMA triblock copolymer.[31] But the low diffusion rates of viscous rubber in the polymer/rubber/filler ternary blend and the micellization or self-assembly effect of copolymers in the copolymer toughened system will limit the formation of effective core−shell structures and make it necessary to increase the rubber content to a relatively high level in order to achieve satisfactory toughness. Furthermore, prior-prepared end-functional block copolymers are neither economical nor practical for large scale productions. In this study, we report a facile method to prepare superductile PA6 that is toughened by core−shell particles formed in situ via reactive extrusion. The neat rubber content can be as low as 1.5 wt % in the blend but with an Izod impact energy as high as 1000 J m^{-1}. The effectiveness of Wu's[7] theory and Corté and Leibler's[20] model in predicting the toughness in particle toughened systems is also discussed.

In conventional polymer/rubber/filler ternary blending system, the high viscosity of rubber will block its diffusion in the melt to encapsulate the rigid particles and thus discourage the formation of core−shell structure during processing, even though Harkin's rule[33] is satisfied.[34] In our work, in order to avoid this problem, a low molecular weight functionalized rubber, polybutadiene-*graft*-maleic anhydride (PB-*g*-MAH) (Yanshan Petro. & Chem. Co.; MAH content = 9−11 wt %, M_w = 3120, polydispersity index = 2.02), was first grafted onto

Scheme 1. Formation of Core−Shell Structures in PA6 Matrix

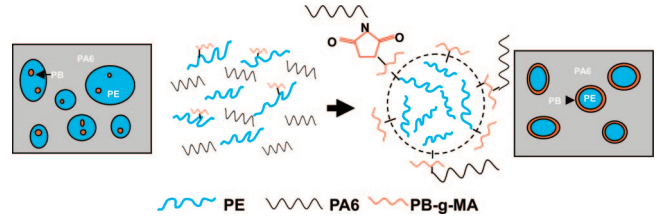

* Corresponding authors.
[†] Graduate University of Chinese Academy of Sciences.
[‡] Hubei University.
[§] City University of Hong Kong.
[||] The University of Sydney.

10.1021/ma800495t CCC: $40.75
Published on Web 09/27/2008

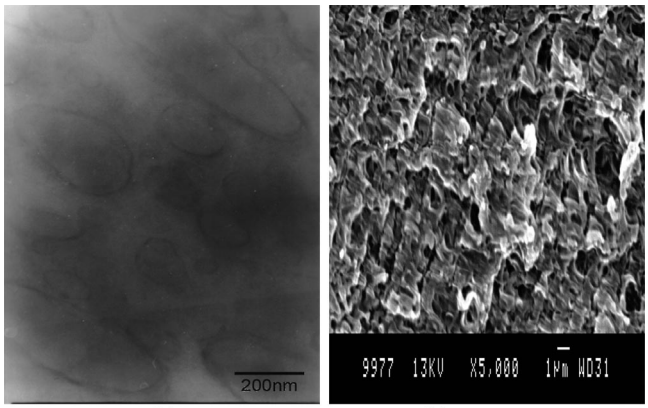

Figure 1. Micrographs of blend 3 [PA6 content 70 wt %]: (a) TEM image stained by OsO_4 and (b) SEM image of impact fracture surface.

a low density polyethylene (LDPE) (Jilin Petro. & Chem. Co., MFI = 2.1 g/10 min at 190 °C) molecule backbone via reactive extrusion with dicumyl peroxide (DCP) as an initiator at 200 °C. The weight composition of LDPE/PB-*g*-MAH/DCP is 95/5/0.1. A selected amount of rubber modified LDPE (LDPE-*g*-PB-*g*-MAH) was then melt-mixed with PA6 at 230 °C. From the reaction between MAH and the amino group in the chain ends of PA6, LDPE-*g*-PB-*g*-PA6 copolymers were formed, which yielded a core−shell structure with a LDPE core and an elastic PB shell in PA6 matrix as shown in Scheme 1. The formation of the core−shell structure in LDPE-*g*-PB-*g*-MAH/PA6 blend (blend 3) (PA6 content is 70 wt %) can be confirmed by the TEM micrograph in Figure 1a. Here, the sample was stained by OsO_4 so that the dark rubber shell (PB-*g*-MAH) around the gray PE particles can be clearly identified. Further, from the SEM micrograph of impact fracture surface, Figure 1b, we can see substantial matrix ductile tearing confirming the high energy dissipated during impact fracture. The mechanical properties of LDPE-*g*-PB-*g*-MAH toughened PA6 are given in Table 1 with those of other PA6 systems toughened by MAH functionalized LDPE (LDPE-*g*-MAH) (blend 1) and polyolefin elastomer-*graft*-maleic anhydride (POE-*g*-MAH) as tougheners (blend 2). Both blend 1 and blend 2 were also prepared by melt mixing with specified amounts of PE-*g*-MAH and POE-*g*-MAH with PA6 at 230 °C. Tensile and Izod impact specimens were prepared by injection molding, and all these specimens were stored in open air at room temperature (~23 °C) for at least 24 h before testing. The data shown in Table 1 are the average values of five measurements. Obviously, the Izod impact energies of these three systems are much improved compared to neat PA6. Also, the impact energies of blend 3 are much higher than blend 1 and blend 2 at identical PA contents. These results show that the thin rubber layer around the LDPE core is much more effective than pure LDPE or POE particles to initiate matrix yielding and dissipate impact energy.

Table 2. Comparisons of Interparticle Ligament Thickness *L* and Critical Interparticle Distance L_C Based on Corté and Leibler's Model[20] for Different Blends

				$L_C{}^c$ (μm)	
sample	PA6 content (wt %)	d^a (μm)	L^b (μm)	$C = 0.1$	$C = 0.2$
blend 1	90	0.43	0.34	0.18	0.40
	80	0.38	0.16	0.16	0.37
	70	0.24	0.06	0.14	0.27
blend 2	90	0.24	0.19	0.14	0.27
	80	0.22	0.09	0.14	0.26
	70	0.17	0.04	0.13	0.22
blend 3	90	0.48	0.38	0.18	0.41
	80	0.41	0.17	0.17	0.37
	70	0.28	0.07	0.15	0.28

[a] $d = \sum n_i d_i^2 / \sum n_i d_i$. [b] $L = d[(\beta\pi/6\Phi)^{1/3} - 1]$, $\beta = 1.09$. [c] $L_C = \xi^* + d(C\sigma_B/\sigma_Y)^2$, $\xi^* = 0.1$ μm, $\sigma_B = 300$ MPa, $\sigma_Y = 70$ MPa.

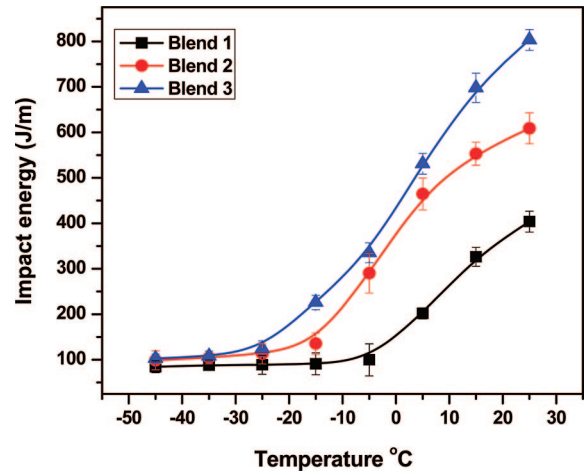

Figure 2. Impact energies of different blends versus temperature (PA6 content 80 wt %).

The dispersed particle size *d* of these blends was calculated from SEM micrographs (not shown here) and listed in Table 2. The interparticle ligament thickness *L* for all these systems are calculated from Wu's[7] equation: $L = d[(\beta\pi/6\Phi)^{1/3} - 1]$, $\beta = 1.09$. It is found that the interparticle ligaments of blend 1 and blend 3 with 90 wt % PA6 in our experiments are larger than 300 nm, which is proposed by Wu[7] as a critical ligament thickness for rubber toughened PA6. Hence, toughening is not expected in these two blends, but the impact energy results in Table 1 suggest otherwise. Moreover, as shown in Table 2, the critical length L_C evaluated using eq 1 due to Corté and Leibler[20] for $\xi^* = 100$ nm is larger than the interparticle ligament thickness *L* for all these blends if $C \geq 0.2$. (The values of ξ^* and *C* used follow those cited in ref 20). So, the model of Corté and Liebler[20] is more suitable than Wu's[7] for predictions of

Table 1. Mechanical Properties of Different Toughened PA6 Blends at 25 °C[a]

sample		Izod impact energy (J m^{-1})	σ_B (MPa)	σ_Y (MPa)	elastic modulus (GPa)
blend 1[b]	PA6 90 wt %	166.2 ± 14.8	65.0 ± 4.4	61.2 ± 1.7	2.22 ± 0.02
	PA6 80 wt %	403.7 ± 19.6	63.2 ± 3.3	57.4 ± 1.6	2.11 ± 0.02
	PA6 70 wt %	512.8 ± 43.2	55.1 ± 3.6	43.3 ± 1.2	1.93 ± 0.05
blend 2[b]	PA6 90 wt %	384.6 ± 30.8	59.3 ± 1.6	50.2 ± 2.0	2.16 ± 0.03
	PA6 80 wt %	608.5 ± 67.5	71.7 ± 1.9	43.8 ± 1.3	2.03 ± 0.07
	PA6 70 wt %	756.4 ± 48.5	96.9 ± 2.3	38.3 ± 1.2	1.67 ± 0.04
blend 3[b]	PA6 90 wt %	630.5 ± 59.7	103.1 ± 7.0	41.7 ± 0.9	2.26 ± 0.05
	PA6 80 wt %	803.0 ± 49.9	151.3 ± 5.0	40.4 ± 0.7	1.92 ± 0.05
	PA6 70 wt %	1003.4 ± 56.4	266.4 ± 6.7	34.3 ± 1.0	1.89 ± 0.06
PA6		64.4 ± 7.0	255.6 ± 1.0	63.3 ± 1.5	2.54 ± 0.04

[a] σ_B is true stress at break, σ_Y is yield stress at maximum load, and elastic modulus is initial tangent modulus. [b] Blend 1: LDPE-*g*-MAH/PA6; blend 2: POE-*g*-MAH/PA6; blend 3: LDPE-*g*-PB-*g*-MAH/PA6.

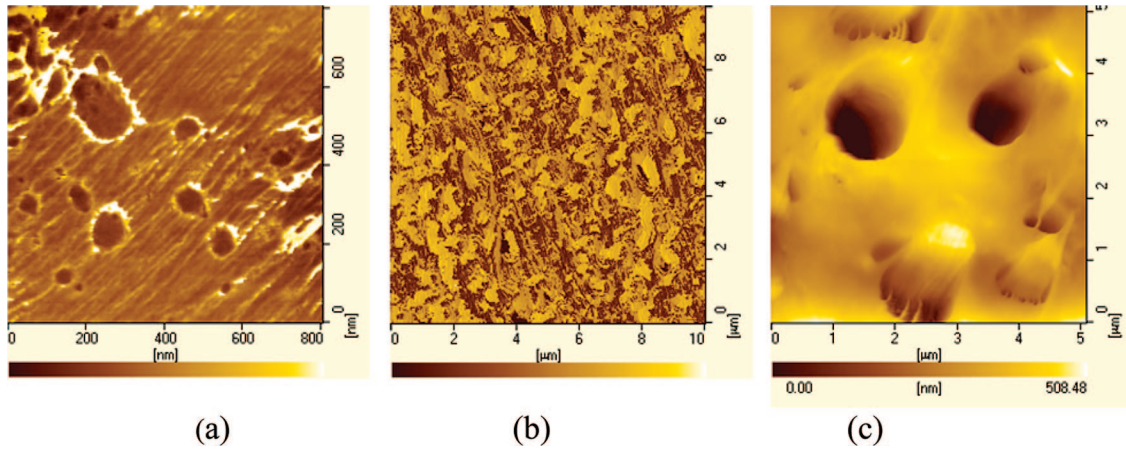

Figure 3. AFM micrograghs of cryo-fractured surface of different blends (PA6 content 80 wt %): (a) blend 1, (b) blend 2, and (c) blend 3.

onset of toughening in these materials. However, this model is still unable to predict the differential toughening effect between blends 1, 2, and 3 containing the same filler content. From eqs 1 and 2, it is apparent that toughening can be more readily achieved if C is larger, since then L_C is higher and Φ_C is lower. Following Corté and Liebler's theory,[20] the brittle−ductile transition temperature, T_{BD}, of these toughened blends can be calculated by

$$T_{BD} = \frac{Y_0}{Y_1(\dot{\varepsilon})} - \frac{C\sigma_B}{Y_1(\dot{\varepsilon})}\left[\left(\frac{\beta\pi}{6\Phi}\right)^{1/3} - 1 - \frac{\xi^*}{d}\right]^{-1/2} \quad (3)$$

where Y_0 and $Y_1(\dot{\varepsilon})$ are characteristic parameters of Eyring's equation:[35] $\sigma_Y(\dot{\varepsilon},T) = Y_0 - Y_1(\dot{\varepsilon})T$ for PA6. Figure 2 shows the impact energies of blends 1, 2, and 3 with 80 wt % PA6 versus temperature. It is seen that T_{BD} of these blends follows the trend $T_{BD(blend3)} < T_{BD(blend2)} < T_{BD(blend1)}$. On the basis of eq 3, for a given polymer matrix and under the same testing conditions, where Y_0 and $Y_1(\dot{\varepsilon})$ are assumed constant, T_{BD} can only be reduced by increasing C or decreasing d. However, as shown in Table 2, the dispersed particle size d for blend 3 is largest among the three blends, that is, $d_{blend3} > d_{blend1} > d_{blend2}$. Hence, the lowest T_{BD} for blend 3 can only be obtained with the highest C value.

In reality, the importance of the parameter C, although related to the cavitational process, should not be overemphasized except that it seems to be a good indicator of the effectiveness of the toughener. Therefore, the larger C is, the better the toughness. Supporting evidence is also given in Figure 3, which shows typical AFM micrographs of cryo-fracture surfaces of these three toughened blends with 80 wt % PA. Interface debonding between LDPE-*g*-MAH and PA6 is easily observed in blend 1 in Figure 3a. The very good interface adhesion seen in Figure 3b suggests that internal cavitation of rubber mostly happens during fracture[30] in blend 2. Finally, as revealed in Figure 3c for blend 3, fibrils are seen at the debonded interface between the core−shell particles and matrix. Similar observations have also been found in other ternary blends with core−shell fillers.[36] In blend 1 and blend 2, interface debonding and internal cavitation indicate that no stresses can be transferred effectively between particles and matrix. However, in blend 3, stresses can be transferred via the fibrils at the interface, and the molecule chains of PA6 connected with these fibrils will be highly elongated during the deformation of the specimen. It is well-known that when a specimen is stretched below the matrix glass transition temperature, T_g, the forced high elasticity,[37,38] that is, the orientation of amorphous molecule chains along the force

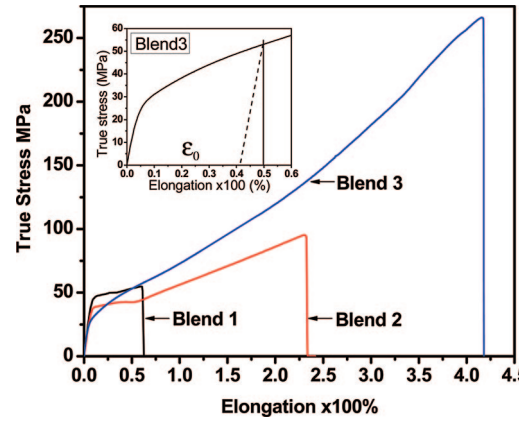

Figure 4. True stress−engineering elongation curves of different blends (PA6 content 70 wt %): blend 1, blend 2, and blend 3.

Table 3. Variation of Crystallinity and Recoverable Forced High Elasticity of Different Blends after Tensile Testing

sample (PA6 70 wt %)	crystallinity (%)		ε_0 (%)	ε_1 (%)	recoverable forced high elasticity $\Delta\varepsilon$ (%)[a]
blend 1	28.22	before drawing	40.6	34.1	15.9
	28.56	after drawing to break			
blend 2	27.09	before drawing	41.0	29.4	28.4
	28.29	after drawing to break			
blend 3	28.75	before drawing	41.2	24.7	40.0
	32.18	after drawing to break			

[a] $\Delta\varepsilon = (\varepsilon_0 - \varepsilon_1)/(\varepsilon_0)$, where ε_0 is necking strain and ε_1 is residual strain after annealing at 80 °C for 12 h.

direction, occurs before or during matrix yielding. In semicrystalline polymers, the forced high elasticity of the deformation of tie chains[39] between crystal lamellae is retractable after annealing the specimen above its T_g provided that these oriented molecule chains do not recrystallize. In our tests, the specimens were first elongated to a necking strain, ε_0 (see inset of Figure 4). Then, they were annealed at 80 °C for 12 h and the residual strains ε_1 recorded. The recoverable forced high elasticity $\Delta\varepsilon$ is defined by $\Delta\varepsilon = (\varepsilon_0 - \varepsilon_1)/\varepsilon_0$, and the results are shown in Table 3. Physically, this represents the recovered elastic strain subjected to tensile drawing. Although the moisture content after annealing is less than that before annealing (~0.2 wt %), it does not have much effect on the retraction and hence $\Delta\varepsilon$. This is because the annealing temperature (80 °C) is well above T_g of PA6, and it is the primary factor (not moisture) which controls

the mobility of all the oriented amorphous chains and thus the residual strain ε_1.

The recoverable forced high elasticity of blend 3 is clearly much larger than blends 1 and 2. These results indicate that the amorphous regions in PA6 matrix are much more influenced by the core−shell rubber particles in blend 3, which confirms more intense drawing of the PA6 molecular chains in blend 3 during tensile testing. Further elongation of the sample results in recrystallization of these highly oriented molecule chains and thus higher crystallinity after drawing.[40] Although we did not study the crystal form of PA6 around the fillers in these three blends, such as trancrystalline regions formed around rubber particles which, upon rubber cavitation, become mobile and deform plastically imparting high toughness to the polyamide matrix,[41] it is found that the overall crystallinity of PA6 is increased in all three blends after being drawn to failure in tensile tests due to the orientation and recrystallization of amorphous PA6 molecule chains. The crystallinity increase is much smaller in blends 1 and 2 than that in blend 3 where fibrils are formed between the matrix and particles. This is also confirmed by the true stress versus engineering elongation curves in Figure 4 such that both elongation and stress σ_B at break for blend 3 are substantially larger than those of blend 1 and blend 2.

Although the PB rubber shell in blend is quite soft, it does not seem to affect adversely the elastic modulus compared to blends 1 and 2 at the same PA6 content. The same cannot be said about the yield strength σ_Y, which shows a clear degradation effect (see Table 1). Relative to neat PA6, considering both elastic (tangent) modulus and notched impact toughness properties, blend 3, with a core−shell toughener, i.e., rigid core and soft rubber shell, is best among these three blend systems. As expected from previous analyses of toughened systems with similar core−shell particles,[42−44] loss of modulus is unavoidable and compromises must be made. From Table 1, for blend with 90 wt % PA and 10 wt % core−shell toughener, there is only a 10% loss in modulus but a 10-fold increase in impact toughness compared to neat PA6. For many practical purposes, this is acceptable.

In summary, core−shell particles with a rigid core and a soft rubber shell are an effective toughener for semicrystalline polymers. Although there is a slight to moderate modulus loss over the range of filler content studied in this toughened material system (blend), supertough materials with low T_{BD} can be obtained with very low rubber content (e.g., the lowest neat rubber content is 0.5 wt %).

Acknowledgment. This work was supported by the NSFC (Nos. 50833005, 50373011, 50673024, and 50390090) and the Research Grants Council of the Hong Kong Special Administrative Region, China (Project No. CityU 117205). D.S. was a Visiting Scholar to the Centre for Advanced Materials Technology (CAMT) at the University of Sydney supported by the Australian Research Council.

References and Notes

(1) Epstein, B. N. U.S. Patent 4, 172, 895, **1979**.
(2) Kinloch, A. J.; Young, R. J. *Fracture Behavior of Polymers*, 2nd ed.; Elsevier Applied Science: London, 1985.
(3) Keskkula, H.; Paul, D. R. Toughened nylons. In *Nylon Plastics Handbook*; Kohan, M. I., Ed.; Hanser: Munich, 1995; pp 414−434.
(4) Koning, C.; Van Duin, M.; Pagnoulle, C.; Jérôme, R. *Prog. Polym. Sci.* **1998**, *23*, 707–757.
(5) Akkapeddi, M. K. Rubber toughening of polyamides by reactive blending. In *Reactive Polymer Blending*; Baker, W., Scott, C. E., Hu, G.-H., Eds.; Hanser: Munich, 2001; p 207.
(6) Borggreve, R. J. M.; Gaymans, R. J.; Schuijer, J.; Ingen Housz, J. F. *Polymer* **1987**, *28*, 1489–1496.
(7) Wu, S. *Polymer* **1985**, *26*, 1855–1863.
(8) Borggreve, R. J. M.; Gaymans, R. J.; Eichenwald, H. M. *Polymer* **1989**, *30*, 78–83.
(9) Muratoglu, O. K.; Argon, A. S.; Cohen, R. E.; Weinberg, M. *Polymer* **1995**, *36*, 4787–4795.
(10) Van der Wal, A.; Gaymans, R. J. *Polymer* **1999**, *40*, 6067–6075.
(11) Argon, A. S.; Cohen, R. E. *Polymer* **2003**, *44*, 6013–6032.
(12) Fukui, T.; Kikuchi, Y.; Inoue, T. *Polymer* **1991**, *32*, 2367–2375.
(13) Lazzeri, A.; Bucknall, C. B. *Polymer* **1995**, *36*, 2895–2902.
(14) Tzika, P. A.; Boyce, M. C.; Parks, D. M. *J. Mech. Phys. Solids* **2000**, *48*, 1893–1929.
(15) Oshinski, A. J.; Keskkula, H.; Paul, D. R. *Polymer* **1996**, *37*, 4919–4928.
(16) Kayano, Y.; Keskkula, H.; Paul, D. R. *Polymer* **1998**, *39*, 2835–2845.
(17) Oshinski, A. J.; Keskkula, H.; Paul, D. R. *Polymer* **1996**, *37*, 4891–907.
(18) Oshinski, A. J.; Keskkula, H.; Paul, D. R. *Polymer* **1996**, *37*, 4919–28.
(19) Okada, O.; Keskkula, H.; Paul, D. R. *Polymer* **1999**, *40*, 2699–709.
(20) (a) Corté, L.; Leibler, L. *Macromolecules* **2007**, *40*, 5606–5611. (b) Modic, M. J.; Pottick, L. A. *Polym. Eng. Sci.* **1993**, *33*, 819–827.
(21) Lazzeri, A.; Bucknall, C. B. *J. Mater. Sci.* **1993**, *28*, 6799–6808.
(22) Yu, Z. Z.; Ou, Y. C.; Qi, Z. N.; Hu, G. H. *J. Polym. Sci., Part B: Polym. Phys.* **1998**, *36*, 1987–1994.
(23) Bai, S. L.; G'Sell, C.; Hiver, J. M.; Mathieu, C. *Polymer* **2005**, *46*, 6437–6446.
(24) Yang, H.; Zhang, Q.; Guo, M.; Wang, C.; Du, R. N.; Fu, Q. *Polymer* **2006**, *47*, 2106–2115.
(25) Premphet, K.; Horanont, P. *Polymer* **2000**, *41*, 9283–9290.
(26) Modic, M. J.; Pottick, L. A. *Polym. Eng. Sci.* **1993**, *33*, 819–827.
(27) Tanrattanakul, V.; Hiltner, A.; Baer, E.; Perkins, W. G.; Massey, F. L.; Moet, A. *Polymer* **1997**, *38*, 2191–2200.
(28) Bassani, A.; Pessan, L. A. *J. Appl. Polym. Sci.* **1997**, *86*, 3466–3479.
(29) Corté, L.; Rebizant, V.; Hochstetter, G.; Tournilhac, F.; Leibler, L. *Macromolecules* **2006**, *39*, 9365–9374.
(30) Sferrazza, M.; Donald, A. M.; Crawshaw, J.; Narayanan, T. *Macromolecules* **2001**, *34*, 6708–6718.
(31) Koulic, C.; Yin, Z.; Pagnoulle, C.; Jérôme, R. *Angew. Chem., Int. Ed.* **2002**, *41*, 2154–2157.
(32) Koulic, C.; François, G.; Jérôme, R. *Macromolecules* **2004**, *37*, 5317–5322.
(33) Harkins, W. D. *The Physical Chemistry of Surface Films*; Reinhold Pub. Co. New York, 1952; p 23.
(34) Horiuchi, S.; Matchariyakul, N.; Yase, K.; Kitano, T.; Cho, H. K.; Lee, Y. M. *Polymer* **1996**, *37*, 3065–3078.
(35) Ward, I. M.; Hadley, D. W. In *Mechanical Properties of Solid Polymers*; Wiley: New York, 1983.
(36) Kim, G. M.; Michler, G. H.; Rösch, J.; Mülhaupt, R. *Acta Polym.* **1998**, *49*, 88–95.
(37) Kozlov, G. V.; Beloshenko, V. A.; Gazaev, M. A.; Novikov, V. U. *Mech. Compos. Mater.* **1996**, *32*, 186–191.
(38) Vlasov, S. V.; Kuleznev, V. N. *Polym. Eng. Sci.* **2004**, *35*, 173–179.
(39) Seguela, R. *J. Polym. Sci., Part B* **2005**, *43*, 1729.
(40) Keller, A. *Rep. Prog. Phys.* **1968**, *31*, 623.
(41) Dasari, A.; Yu, Z. Z.; Mai, Y.-W. *Macromolecules* **2007**, *40*, 123–130.
(42) Matonis, V. A.; Small, N. C. *Polym. Eng. Sci.* **1969**, *9*, 90–99.
(43) Matonis, V. A.; Small, N. C. *Polym. Eng. Sci.* **1969**, *9*, 100–104.
(44) Cherkaoui, M.; Sabar, H.; Berveiller, M. *J. Eng. Mater. Tech.* **1994**, *116*, 274–278.

MA800495T